

SUPPLEMENTARY MATERIAL FOR:

Distribution of charged residues affects the average size and shape of intrinsically disordered proteins

Greta Bianchi¹, Marco Mangiagalli¹, Alberto Barbiroli², Sonia Longhi³, Rita Grandori¹, Carlo Santambrogio^{1*}, Stefania Brocca^{1*}

¹Dept. of Biotechnology and Biosciences, University of Milano-Bicocca, 20126, Milan, Italy

²Dept. of Food, Environmental and Nutritional Sciences, University of Milan, 20133, Milan, Italy

³Lab. Architecture et Fonction des Macromolécules Biologiques (AFMB), UMR 7257, Aix-Marseille University and CNRS, 13288, Marseille, France

* Correspondence:

Prof. Stefania Brocca, Department of Biotechnology and Biosciences, University of Milano-Bicocca, Piazza della Scienza 2, 20126 Milan, Italy.

Phone: 0264483518

E-mail: stefania.brocca@unimib.it;

Dr. Carlo Santambrogio, Department of Biotechnology and Biosciences, University of Milano-Bicocca, Piazza della Scienza 2, 20126 Milan, Italy.

Phone: 0264483363

E-mail: carlo.santambrogio@unimib.it

Table S1. Size of the semi-axes of ellipsoids assimilated to the model proteins studied in this work

Protein variant		<i>a</i> (nm)	<i>b</i> (nm)	<i>c</i> (nm)	Surface* (nm ²)
N _{TAIL}	Low κ	3.00 ± 0.03	2.21 ± 0.03	1.78 ± 0.04	67.5 ± 1.9
	wt	2.90 ± 0.02	2.17 ± 0.03	1.76 ± 0.03	64.4 ± 1.5
	High κ	2.67 ± 0.01	2.02 ± 0.04	1.66 ± 0.06	55.8 ± 2.1
NFM	Low κ	3.29 ± 0.02	2.83 ± 0.04	2.54 ± 0.07	104.5 ± 3.4
	wt	3.15 ± 0.03	2.78 ± 0.04	2.54 ± 0.07	100.0 ± 3.3
	High κ	2.55 ± 0.01	2.62 ± 0.02	2.49 ± 0.09	81.9 ± 6.2
PNT4	Low κ	2.92 ± 0.04	1.69 ± 0.07	1.36 ± 0.03	48.1 ± 2.3
	wt	2.91 ± 0.04	1.64 ± 0.08	1.34 ± 0.03	46.8 ± 2.4
	High κ	2.34 ± 0.02	1.89 ± 0.05	1.61 ± 0.07	47.4 ± 2.3

* calculated by Thomsen's approximation (maximal discrepancy ~1%)

N_{TAIL}

Low-k	MHHHHHHTT ERD ISRAVG PD QAQVSFLHG KQSENRLPELGGKEKERV DQSRGEARESY ED	60
wt	MHHHHHHTT EDK ISRAVG PR QAQVSFLHG DQSENRLPRLGGKEDRRVKQSRGEARESYRE	60
High-k	MHHHHHHTT RKR ISRAVG PR QAQVSFLHG RQSRNRLPRLGGKRKRRVRQSRGRAD ESY ED	60
Low-k	TG PS RAS D ARAAHL PTGTPLD IDTAS RSSQDPQRS ERSADALLRLQAMAGIS ERQGS DT D	120
wt	TG PS RAS D ARAAHL PTGTPLD IDTAS ESSQDPQDSRR SADALLRLQAMAGIS EEQGS DT D	120
High-k	TG PS EAS D AEAAHL PTGTPLD IDTAS ESSQDPQDS EESADALL EL QAMAGIS EDQGS DT D	120
Low-k	T PI VYN DR NLL D GS	134
wt	T PI VYN DR NLL D GS	134
High-k	T PI VYN DE NLL D GS	134

NFM

Low-k	MHHHHHH D GAKGS DKEK IAVNG EV EGKEE VKQETKEK SG DEREK GVVTNGL DLS PAKEK	60
wt	MHHHHHH K GAKGS RKED IAVNG EV EGKEE EQETKEK SG REEEK GVVTNGL DLS PADEK	60
High-k	MHHHHHH K GAKGS RKKK IAVNG KVKGKKV KQKT KKK SG RKKKK GVVTNGL KLS PAKED	60
Low-k	E GG DKS EEKVVVT ETV EKITS EGGR GATE EYITK SVTVTQ EVKEHKE TF KEK LVST EKVEK	120
wt	K GG DKS EEKVVVT KTVE KITS EGGD GAT KYITK SVTVTQ KVEEHEE TF EKE LVST KKVEK	120
High-k	D GG DE SEEEVVVT ETVEE ITS EGGD GATE EYITK SVTVTQ VEEHEE TF EEEL VST EEVED	120
Low-k	VTSHAIV EK VTQSD D GS	136
wt	VTSHAIV KE VTQSD D GS	136
High-k	VTSHAIV EE VTQSD D GS	136

PNT4

Low-k	MHHHHHH KETPRVDR KS LMQD SC KEGGVPER LP MLSREF RCSGS DRPIIQELREK GSH P	60
wt	MHHHHHH EETPDVRR KD SLMQD SC KRGGVPKRL P MLSEEF ECSGS DDPIIQELE REGSH P	60
High-k	MHHHHHH KRTPRVRR KS LMQR SC KRGGVPKRL P MLSRKF RCSGS KRPIIQRL ED EGSH P	60
Low-k	GGSL DLREPP QSSGNS RNQPD RQLKT GDAAS P GGVQRP GT PMPKS EIM PIKE GS	114
wt	GGSL RLREPP QSSGNS RNQPD RQLKT GDAAS P GGVQRP GT PMPKS RIM PIK GS	114
High-k	GGSL ELEPP QSSGNS ENQPD EQLD TGDAAS P GGVQEP GT PMPDS EIM PID GS	114

Figure S1. Amino acid sequences of model IDPs. The wt, low- κ and high- κ variants within each of the three sets have been aligned to highlight the sequence design. Positively charged residues are shown in blue, negatively charged residues in red, yellow highlights proline residues. Sequence alignments were carried out with Clustal Omega (Sievers et al, 2011, doi:10.1038/msb.2011.75)

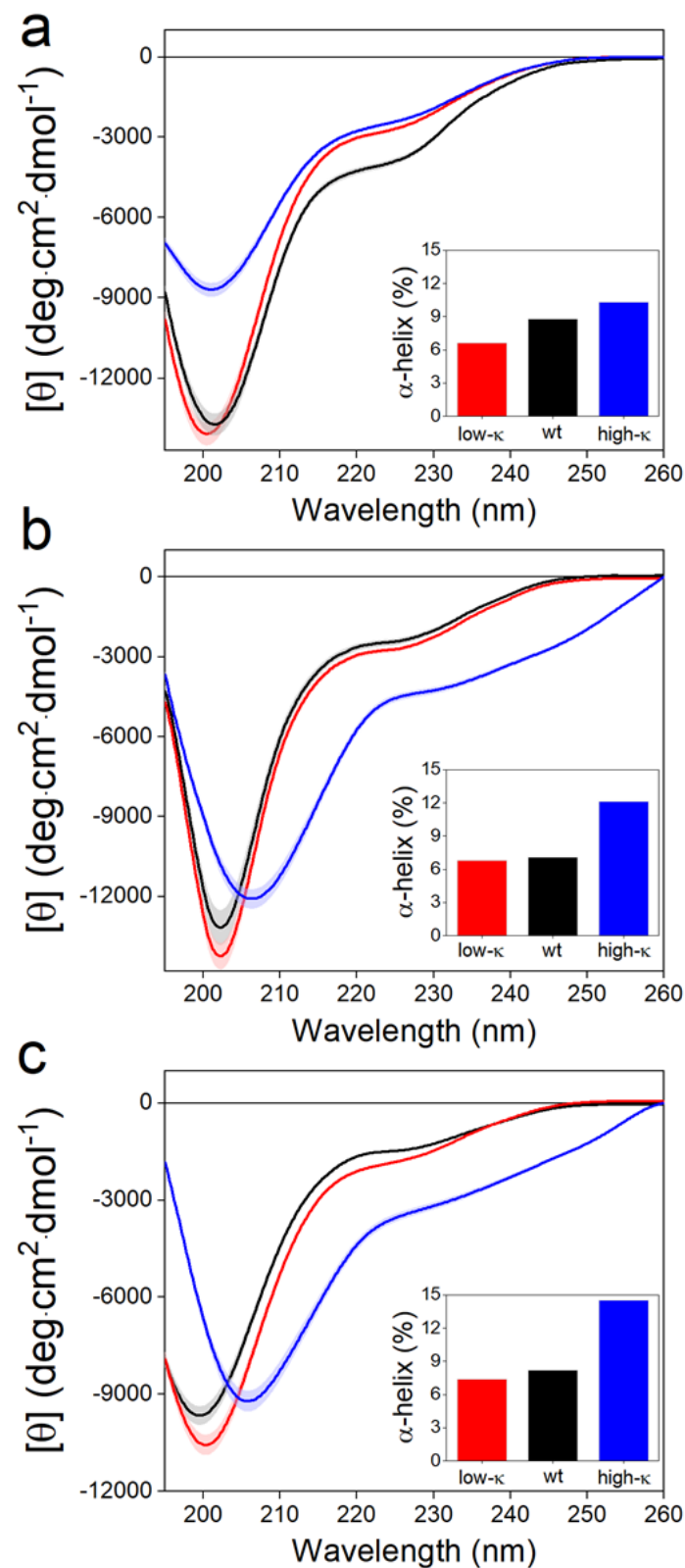


Figure S2. Far-UV CD spectra of model IDPs. CD spectra of N_{TAIL} (a), NFM (b), and PNT4 (c) variants. CD analyses were performed in PBS. The shadowed area refers to the standard deviation of three independent measurements. In black the spectrum of wt proteins, while red and blue are used for the spectra of low- κ and high- κ permutants, respectively. Inset of each panel: percentage of α -helical content as estimated by BeStSel software (Micsonai et al., 2018; doi:10.1093/nar/gky497).

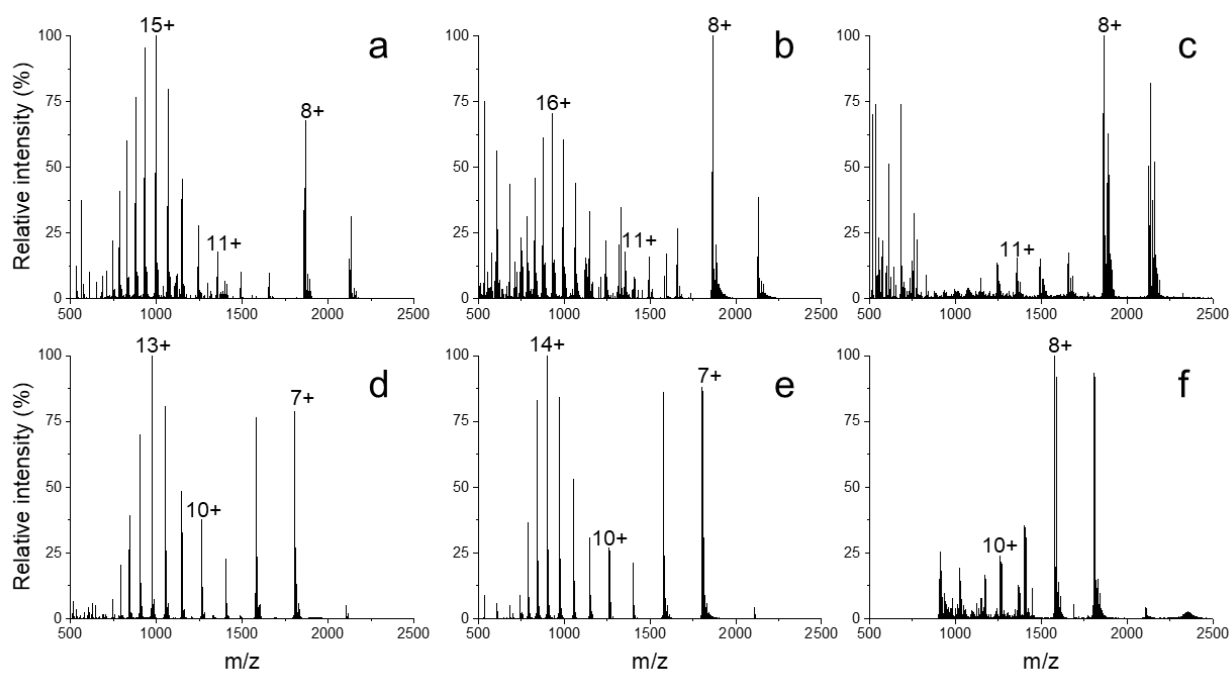


Figure S3. Native MS analyses of model IDPs. NanoESI-MS spectra of NFM (a-c) and PNT4 (d-f) variants acquired under non-denaturing conditions (50 mM ammonium acetate, pH 7.0). Low- κ variants (a, d), wt variants (b, e) and high- κ variants (c, f) are reported.

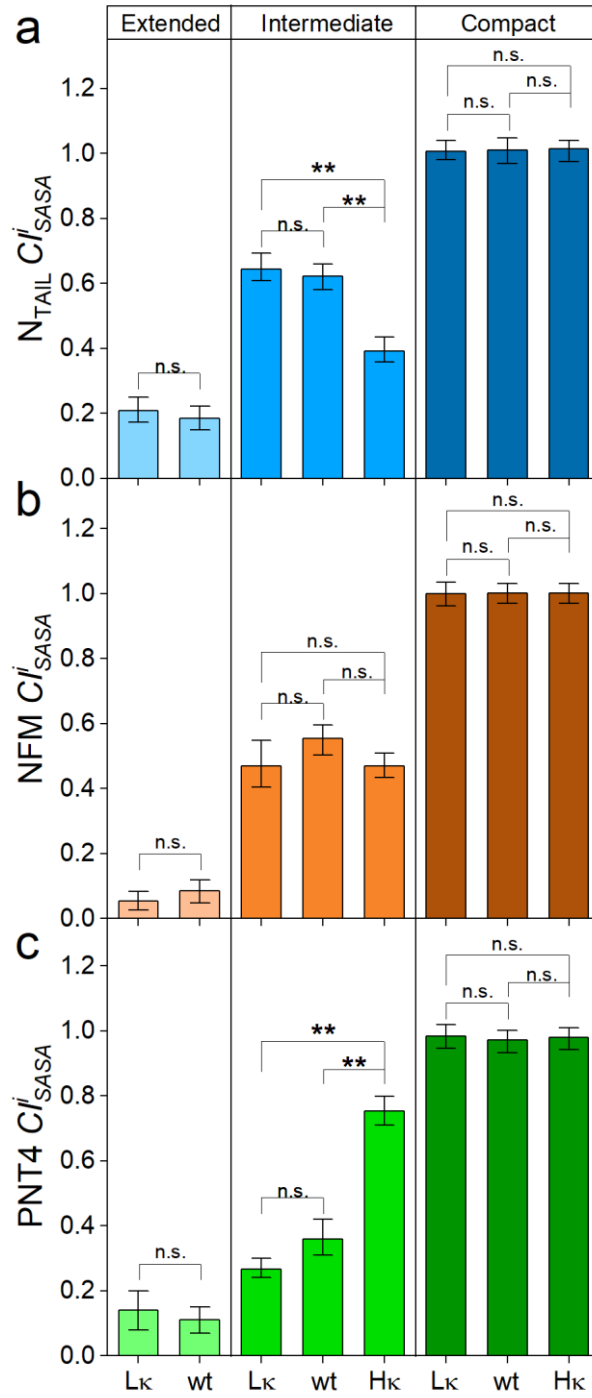


Figure S4. Compactness of conformational components of model IDPs studied by native MS. Bar chart reporting CI_{SASA}^i of N_{TAIL} (a), NFM (b) and PNT4 (c). Mean values of three independent measurements are shown with error bars indicating standard deviations. Statistical analyses were carried out using Welch's t-test (n.s.: $p > 0.05$, *: $p < 0.05$, **: $p < 0.01$).

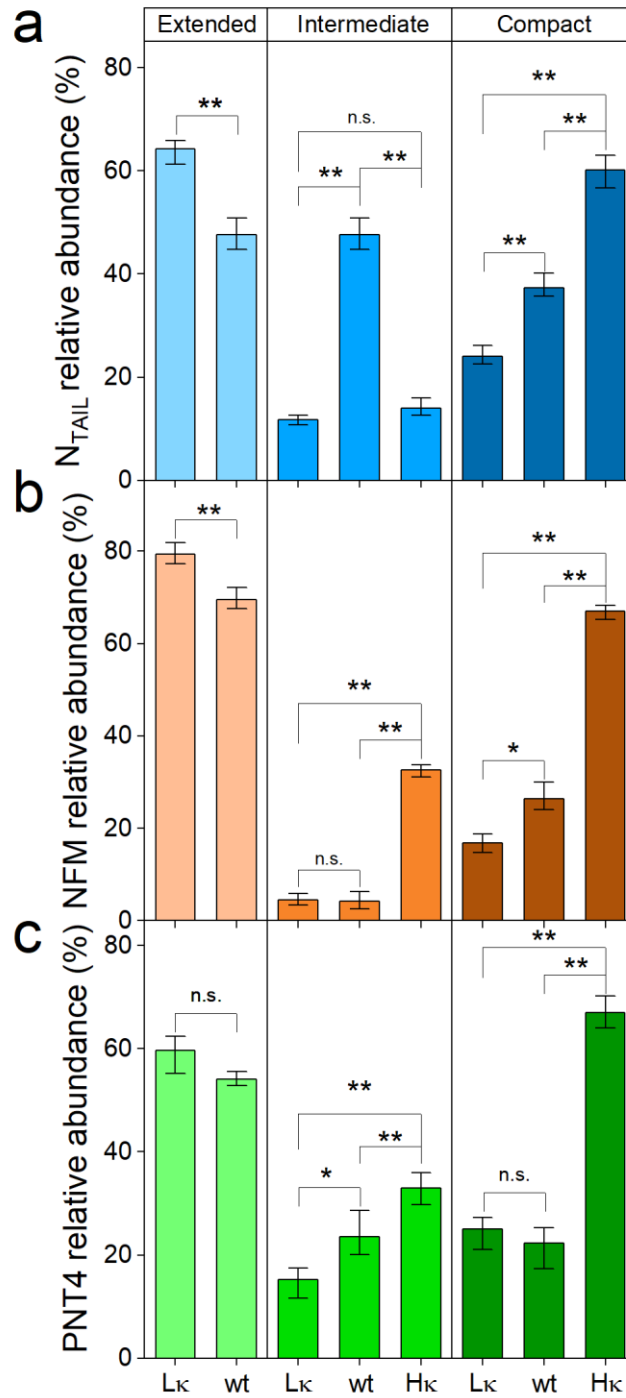


Figure S5. Relative abundance of conformational components of model IDPs studied by native MS. Bar chart reporting the relative abundance of single conformational components (extended; intermediate; compact) of N_{TAIL} (a), NFM (b) and PNT4 (c). Mean values of three independent measurements are represented with error bars indicating standard deviations. Statistical analyses were carried out using Welch's t-test ($p > 0.05$ n.s., * $p < 0.05$, ** $p < 0.01$).

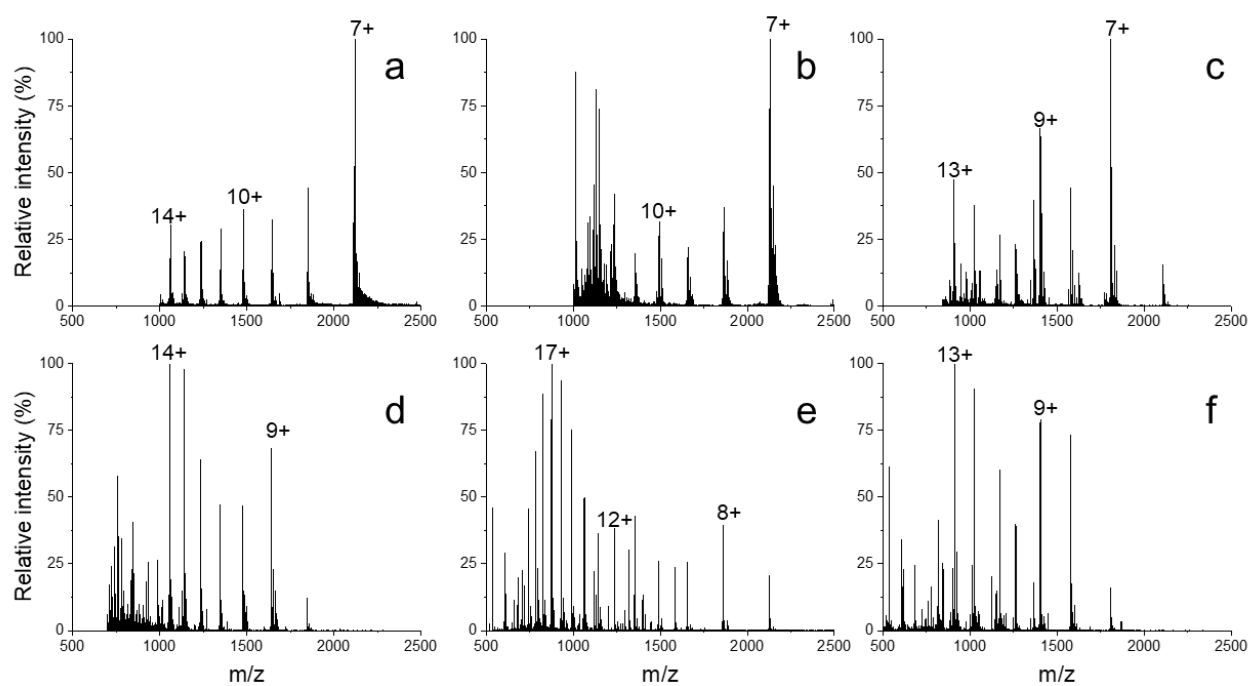


Figure S6. NanoESI-MS spectra of model IDPs under conditions affecting electrostatic interactions. NanoESI-MS spectra of high- κ variants of N_{TAIL} (**a**, **d**), NFM (**b**, **e**) and PNT4 (**c**, **f**) acquired in the presence of 200 mM ammonium acetate pH 7.0 (**a-c**), and in the presence of 1% formic acid (**d-f**).